Robust Multivariable Flutter Suppression for the Benchmark Active Control Technology (BACT) Wind-Tunnel Model

Martin R. Waszak
NASA Langley Research Center
Hampton, Virginia

Abstract

The Benchmark Active Controls Technology (BACT) project is part of NASA Langley Research Center's Benchmark Models Program for studying transonic aeroelastic phenomena. In January of 1996 the BACT wind-tunnel model was used to successfully demonstrate the application of robust multivariable control design methods (H∞ and μ-synthesis) to flutter suppression. This paper addresses the design and experimental evaluation of robust multivariable flutter suppression control laws with particular attention paid to the degree to which stability and performance robustness was achieved.

Introduction

Active control of aeroelastic phenomena, especially in the transonic speed regime, is a key technology for future aircraft design.[1] The Benchmark Active Controls Technology (BACT) project is part of NASA Langley Research Center's Benchmark Models Program[1,2] for studying transonic aeroelastic phenomena. The BACT wind-tunnel model was developed to collect high quality unsteady aerodynamic data (pressures and loads) near transonic flutter conditions. Accomplishing this objective required the design and implementation of active flutter suppression. Two spoiler-type control effectors were utilized to investigate the potential for using spoilers to suppress wing flutter. In addition, multiple control surfaces and sensors enabled the investigation of multivariable flutter suppression. An added benefit of multivariable control laws was to provide an opportunity to evaluate the effectiveness of an on-line controller performance evaluation (CPE) tool[3] to assess open- and closed-loop stability robustness of multivariable systems.

The control law designs were performed in two stages. The first stage involved the design and test of single-input/single-output (SISO) controllers to demonstrate and assess the potential for using spoilers to suppress wing flutter. Since similar designs have been successful in the past,[4] this approach also served to reduce the risk of implementing active flutter suppression and thereby increase the probability of achieving the program objectives. The SISO control results also provided a benchmark for evaluating the benefits of multi-input/multi-output (MIMO) control. The second stage involved the design and test of MIMO controllers to demonstrate the potential for enhanced performance and robustness afforded by the robust multivariable design methods.

The design strategy involved using a single fixed control law to suppress flutter over the anticipated range of wind-tunnel operating conditions (rather than using a scheduled control law, for example). This served to simplfy the controller implementation and data analysis, and is representative of how flutter suppression could be effectively implemented on an actual aircraft. This same strategy was applied to both the SISO and MIMO control law designs.

Before the design and analysis of the control laws is discussed a short description of the wind-tunnel model and the mathematical model used for the control design is presented. The design objectives are then discussed followed by discussions of the SISO and MIMO design efforts. Finally, analysis and wind-tunnel test results will be presented.

Presented at the Eleventh Symposium on Structural Dynamics and Control
Virginia Polytechnic Institute and State Univerisy, Blacksburg, Virginia
May 12-14, 1997

The BACT Wind-Tunnel Model

Physical Model

The BACT system consists of a rigid wing section and a flexible mounting system[5] as shown in the photograph in Figure 1. The rigid, rectangular wing has an NACA 0012 airfoil section. It is equipped with a trailing-edge control surface, and upper- and lower-surface spoilers that are controlled independently by hydraulic actuators. The lower spoiler (not visible) is identical in size, shape, and relative location to the upper spoiler. The wing section is instrumented with pressure transducers, accelerometers, control surface position sensors, and hydraulic pressure transducers. The accelerometers are the primary sensors for feedback control and are located at each corner of the wing.

Figure 1 - Photograph of BACT wing section and flexible mount.

The wing is mounted to a device called the Pitch and Plunge Apparatus (or PAPA) which is designed to permit motion in principally two modes -- rotation (or pitch), and vertical translation (or plunge). The PAPA is instrumented with strain gauges to measure normal force and pitching moment and is mounted to a turntable that can be rotated to control the wing angle of attack. During operation the mounting system is isolated from the wing section by a splitter plate and from the air flow by a faring that is secured to the splitter plate and the wall of the test section.

The combination of the BACT wing section and PAPA mount will be referred to as the BACT system. The BACT system was precisely tuned to flutter within the operating range of the NASA Langley Transonic Dynamics Tunnel (TDT)[6] in which the system was tested. The range of Mach number and dynamic pressure over which flutter testing was performed permits the study of transonic aeroelastic phenomena. The transonic flutter dip for the BACT system occurs for a range of Mach numbers from about 0.70 to 0.85. For a Mach number of about 0.77, the flutter frequency is approximately 4 Hz (25.1 rad / sec) and the flutter dynamic pressure is approximately 148 psf. More detailed descriptions of both the BACT wing section and the PAPA mounting system can be found in References 5 and 7.

Mathematical Model

A mathematical model of the BACT system was developed from first principles expressly for application to control system design. The emphasis of the modeling process was to accurately represent the dynamic characteristics of the BACT system in the frequency range near flutter and over a wide range of wind-tunnel operating conditions. The development of the mathematical model is presented in Reference 8. The model includes the structural dynamics, aerodynamics, and actuator dynamics. In addition, a simple model of the wind-tunnel turbulence was developed from

experimental data. The complete state-space design model is parameterized by dynamic pressure and has ten states, the four states associated with the pitch and plunge degrees of freedom, two states each for the trailing edge surface and upper spoiler actuators, and two states associated with the wind-tunnel turbulence. The units on the control inputs are in degrees and the units on the acceleration outputs are in g's. Stability and control derivatives were only available for a single Mach number of 0.77 but produce dynamic response characteristics that are representative of the Mach number range over which the wind-tunnel tests were performed.

The feedback control system for the BACT was implemented with a digital computer running at 200 samples per second. First order 25 Hz antialiasing filters were provided as part of the wind-tunnel model system for each accelerometer channel. These filters provided an acceptable level of attenuation at frequencies beyond the 100 Hz folding frequency and had the virtue of introducing relatively little phase lag at frequencies near flutter. The digital controller implementation also generated a 0.005 second computational delay that introduced additional lag into the system. A third order Pade approximation filter was used to model the effect of the delay.

Flutter Suppression Design

The active flutter suppression design was performed in two phases -- a SISO design phase and a MIMO design phase. This paper will focus on the MIMO designs, however, the SISO designs will be reviewed to provide a basis for comparison.

There were essentially four main design objectives for all the flutter suppression control designs -

- maintain stability over the entire range of operation (robust stability),
- significantly reduce pitch and plunge accelerations at all operating conditions (robust performance),
- minimize required control activity (both deflections and rates),
- use a single, low order controller to simplify implementation and reduce risk.

SISO Designs

Two SISO control laws were designed and implemented -- one controller used the trailing edge flap and the other used the upper spoiler for control. The trailing edge flap control law was designed by Dr. Vivek Mukhopadhyay from NASA Langley Research Center. The design essentially sought to maximize robustness over the range of dynamic pressures using a single, fixed dynamic compensator element and with a fixed blending of the inboard leading and trailing edge accelerometers signals (LEI and TEI, respectively) for feedback. A plot of the control law frequency response is shown in Figure 2(a). A state space representation of the trailing edge control law is shown in Equation (1).

$$\dot{x} = \begin{bmatrix} -10 & 0 & 0 \\ 5 & -5 & 0 \\ 100 & 2 & -5 \end{bmatrix} x + \begin{bmatrix} 0.0488 & -0.0195 \\ 0.0006 & -0.0002 \\ 0.012 & -0.0048 \end{bmatrix} \begin{Bmatrix} \ddot{z}_{TEI} \\ \ddot{z}_{LEI} \end{Bmatrix}$$

$$\delta_{US} = \begin{bmatrix} 1037.2 & 205.0 & -506.0 \end{bmatrix} x + \begin{bmatrix} 3866.0 & -608.0 \end{bmatrix} \begin{Bmatrix} \ddot{z}_{TEI} \\ \ddot{z}_{LEI} \end{Bmatrix} \qquad (1)$$

The upper spoiler SISO controller was designed by the author with essentially the same design approach. In addition, however, a controller was sought for which phase and gain could be altered independently to introduce specific gain and phase variations to assess the ability of the Controller Performance Evaluation (CPE) tool[3] to effectively determine stability margins from experimental response data. This was accomplished by making the controller all-pass. An additional first order high-pass "washout" filter was added to make the controller insensitive to biases and low

frequency disturbances (e.g., amplifier drift in the accelerometer signals). Attenuation at frequencies far above the flutter frequency was provided by the antialiasing filters (and actuator dynamics). A plot of the controller frequency response is shown in Figure 2(b). The high frequency roll-off provided by the antialiasing is not shown. A state space representation of the upper spoiler control law is shown in Equation (2).

$$\dot{x} = \begin{bmatrix} -0.25 & 0 & 0 \\ -0.25 & -13.33 & -59.26 \\ 0 & 1 & 0 \end{bmatrix} x + \begin{bmatrix} 0.9696 & -0.9696 \\ 0.9696 & -0.9696 \\ 0 & 0 \end{bmatrix} \begin{Bmatrix} \ddot{z}_{TEI} \\ \ddot{z}_{LEI} \end{Bmatrix}$$
$$\delta_{US} = \begin{bmatrix} -6.25 & -666.67 & 0 \end{bmatrix} x + \begin{bmatrix} 24.24 & -24.24 \end{bmatrix} \begin{Bmatrix} \ddot{z}_{TEI} \\ \ddot{z}_{LEI} \end{Bmatrix} \quad (2)$$

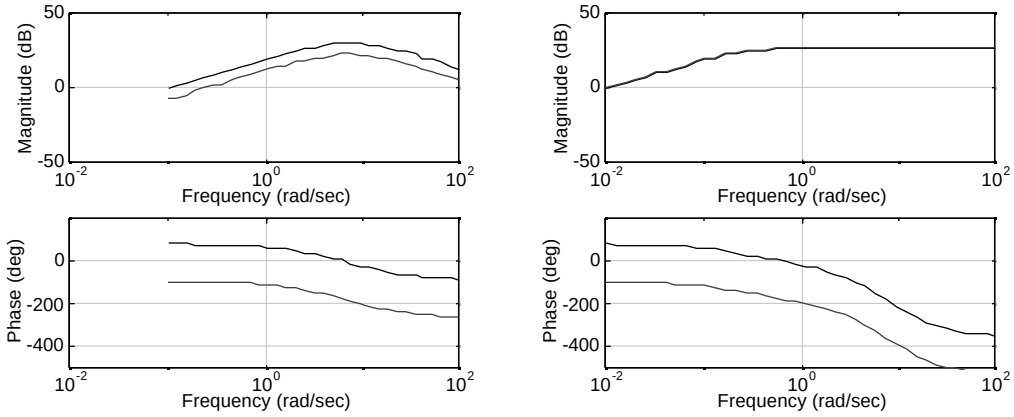

(a) Trailing edge flap control law. (b) Upper spoiler control law.

Figure 2 - Frequency response of SISO controllers
(solid - TEI accel., dash - LEI accel.).

MIMO Designs

The MIMO designs were developed using H-∞ and μ-synthesis design methods. [9,10] These methods produce multivariable control laws that provide stability robustness to modeled uncertainties in the former case and stability and performance robustness to modeled uncertainties in the latter case and are very amenable to flutter suppression applications where robust stability subject to limited control activity is a key requirement. The multivariable control law designs were performed after the SISO designs were implemented and tested on the BACT wind-tunnel model. The MIMO designs benefited greatly from the lessons learned during the SISO design and test phase. In addition, the results of the SISO tests were used to assist in the development of the design specifications for the MIMO control laws.

P-Δ Model Structure

The application of the H-∞ and μ-synthesis methods require a special model structure that isolates key input and output response variables associated with the various performance and robustness requirements. The P-Δ model structure shown in Figure 3 was developed to combine the basic plant dynamics with various weighting functions associated with the required levels of performance, control power, and uncertainty in the plant model. Each of the elements in this structure will be discussed briefly below.

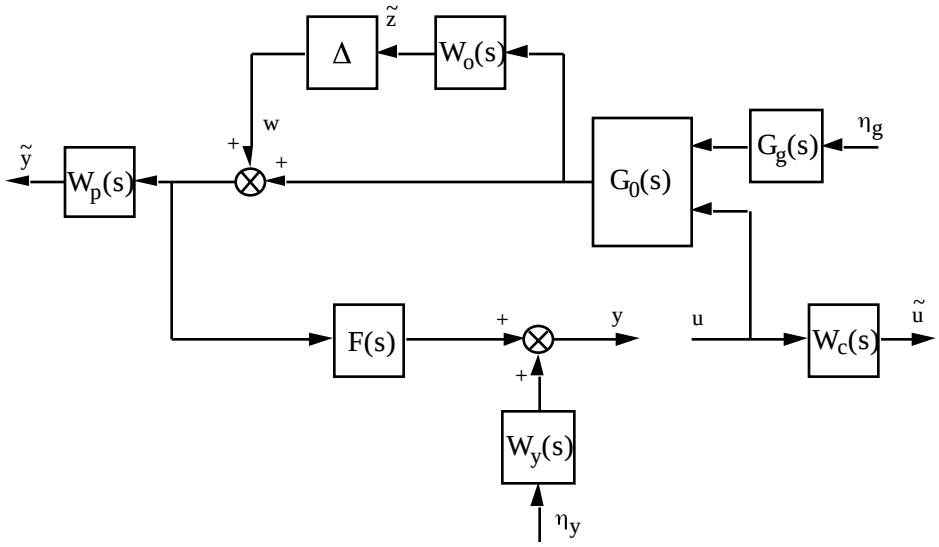

Figure 3 - P-Δ model for the BACT system.

Plant Model

The plant model is associated with three of the block elements in Figure 3 -- the nominal BACT system including actuator dynamics, $G_0(s)$, the turbulence model, $G_g(s)$, and the antialiasing filters and controller time delay approximation, $F(s)$. The turbulence model, $G_g(s)$, and the filters, $F(s)$, were simply state space realizations of the models described in reference 8.

The nominal BACT system model was developed to address the objective to design a single control law that would maintain stability over the entire range of anticipated wind-tunnel operating conditions (Mach and dynamic pressure variations). A model averaging approach[11] was used. This approach generates a single model that passes through the "middle" of the frequency responses of a given ensemble of models and provides a means by which an uncertainty model can be formulated. The model averaging approach was applied to an ensemble of plant models corresponding to the range of dynamic pressures associated with unstable conditions so as not to change the number of right half plane eigenvalues of the perturbed plant relative to the nominal plant.

A key step in the model averaging approach is order reduction since the averaging process results in potentially very high order systems -- the order of the design model multiplied by the number of models in the ensemble. The approach used here differs from that used in reference 11 in that, even though internally balanced reduction was used in both cases, frequency weighting[12] was required to assure that the frequency response of the averaged model had the proper slope at low frequencies. In addition, the reduced order average model was chosen to exhibit two aeroelastic modes like the actual BACT system. As a result, the model that resulted only approximates the true average model. Figure 4 shows a respresentative frequency response plot (trailing edge acceleration due to trailing edge control) for the reduced order average model and the ensemble upon which it is based. The other input-output pairs are similar.

Uncertainty Representation

An unstructured output multiplicative uncertainty model was obtained from the average model and the ensemble. The uncertainty model represents an upper-bound on the maximum singular values of the difference between the average model and the ensemble. A simple fourth order transfer

function was selected so that $|W_o(s)| \geq \bar{\sigma}(\Delta_o) \geq \max_i \left\{ \frac{\bar{\sigma}(G_i(s) - G_0(s))}{\bar{\sigma}(G_0(s))} \right\}$, where i is the number of models in the ensemble. Figure 5 shows the frequency response magnitude for the uncertainty model.

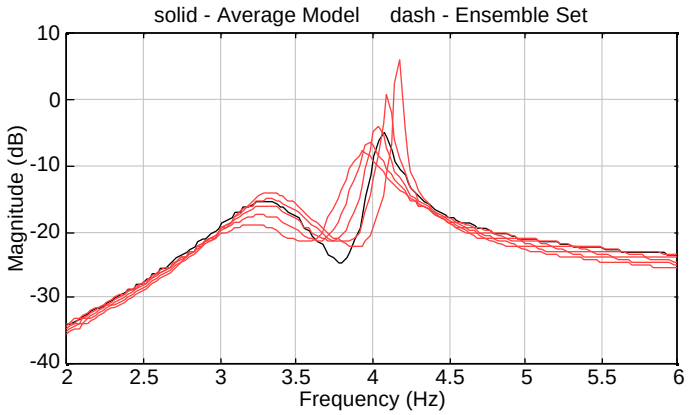

Figure 4 - Averaged design model frequency response compared to ensemble set, (ensemble : M=0.77, q= 155, 165, 175, 185, and 195 psf).

Weighting Functions

The performance, control, and output weighting functions, $W_p(s)$, $W_c(s)$, and $W_y(s)$, respectively, were chosen to achieve similar levels of performance and control activity as was achieved by the SISO controllers. Two sets of performance and control weights were considered -- a simple set chosen primarily to achieve desired acceleration response and control activity, and a more complex set chosen to more precisely shape the frequencies over which the controller would operate.

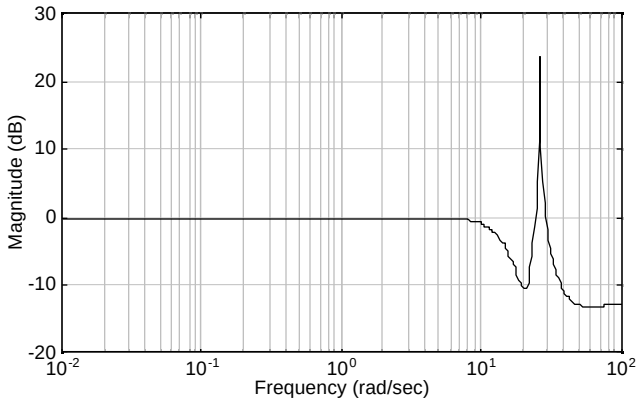

Figure 5 - Uncertainty model frequency response magnitude.

The simple weights set the maximum acceleration level and control deflections over a range of frequencies from zero to beyond the folding frequency. Data from the SISO controller experiments indicated that attenuation to rms levels of 0.03 g's was achievable with rms control activity around 0.3 degrees. The performance weight was chosen so that the peak acceleration level for either pitch or plunge would not exceed 0.1 g's. The control weight was chosen so that peak control deflections of the trailing edge flap and upper spoiler would not exceed 1.0 degree.

The complex weights put more emphasis on keeping control activity limited to the frequencies near flutter by penalizing acceleration and control activity in a narrower frequency band (roughly 1 to 100 rad / sec). The performance weight was chosen as above to keep accelerations below about 0.1 g's. The control weight in this case was less stringent and limited peak deflections to approximately 3.0 degrees. Figure 6 shows the two sets of performance and control weights used in the MIMO designs.

The output weighting function, $W_y(s)$, is required for the H-∞ algorithms to work. The accelerometers were believed to be quite accurate and so the weights were chosen to be a small constant value, 1e-04.

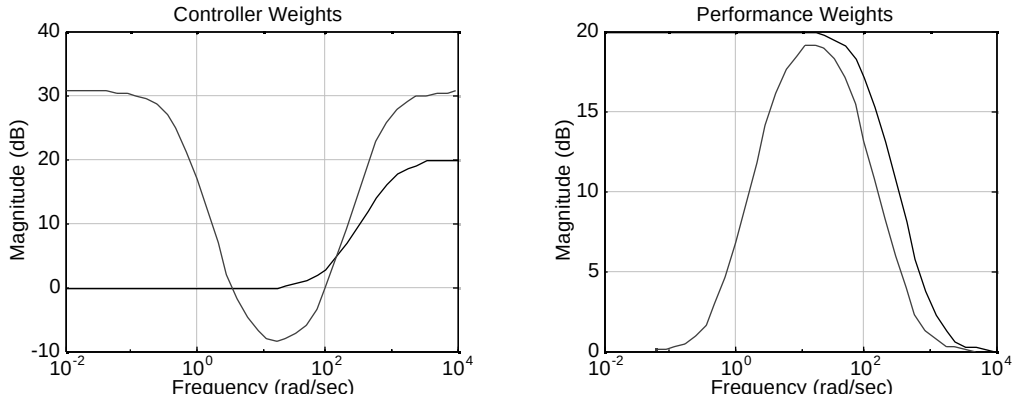

Figure 6 - Performance and control weighting functions for H-∞ and μ-synthesis applications (solid - simple weights, dash - complex weights).

H-∞ Designs

The H-∞ control law designs were computed using the μ-Analysis and Synthesis Toolbox[9] for use with MATLAB. Two controllers were designed with the H-∞ approach using the plant model, the two sets of performance and control weights, and output weight mentioned above. However, the design algorithm was unable to obtain a control law when the uncertainty model derived from the average plant model was used. As a result, a simple unit-ball uncertainty, $W_O(s) = 1$, was used instead and resulted in acceptable designs.

Once the control laws were obtained washout filters (identical to those used for the SISO spoiler control law) were added to make the controller insensitive to biases and low frequency disturbances. The added washout filters were required even for the design based on the complex weights because sufficient attenuation (especially near zero frequency) could not be achieved. This was particularly important since the amplifiers associated with the accelerometers used for feedback exhibited significant bias and low frequency drift.

Control law H-∞ #1, based on the simple weights, was 29th order. Control law H-∞ #2, based on the complex weights, was 37th order. The addition of two first order washout filters further increased the controller order by two. Both of these control laws were too large to fit within the digital controller. As a result, controller order reduction was employed to reduce the order. Internally balanced reduction[12] was used to reduce the model order without sacrificing frequency response accuracy near flutter (1 to 10 hertz). The final order for control laws H-∞ #1 and H-∞ #2 were 7 and 12, respectively. Figures 7 and 8 depict the frequency responses of the two reduced order control laws that were tested in the wind-tunnel.

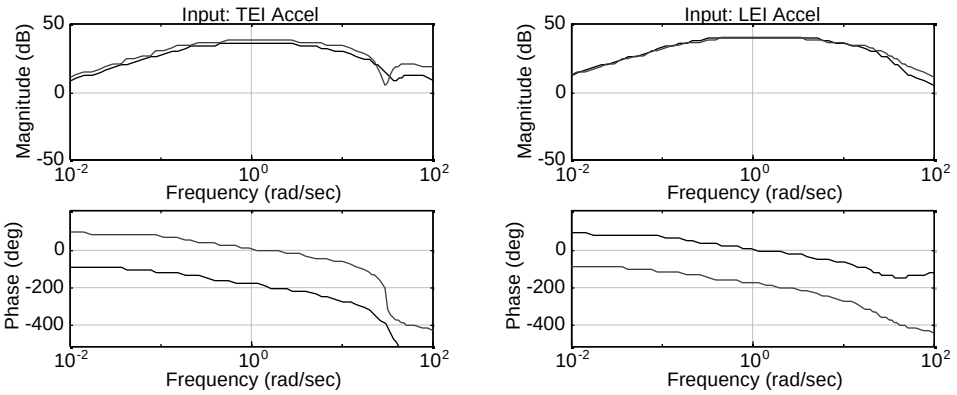

Figure 7 - H-∞ #1 frequency responses (solid - TE control, dash - US control).

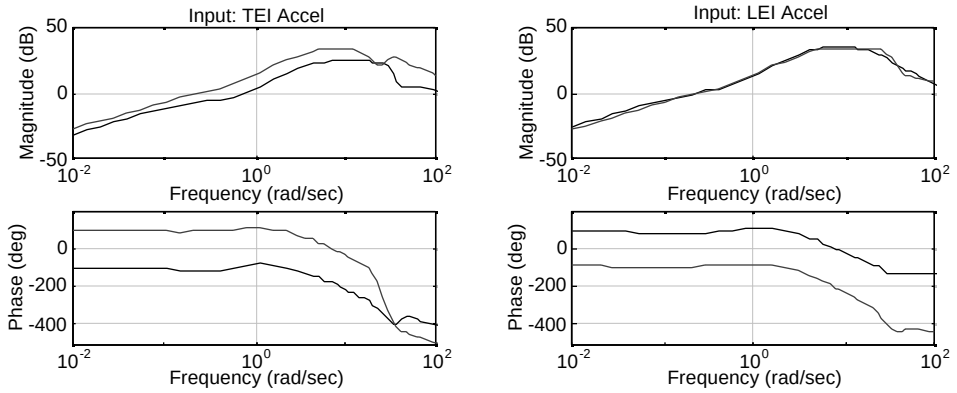

Figure 8 - H-∞ #2 frequency responses (solid - TE control, dash - US control).

μ-Synthesis Designs

The μ-synthesis control law designs were also computed using the μ-Analysis and Synthesis Toolbox.[9] Three controllers were designed with the μ-synthesis approach using the same plant model and performance, control, output, and unit-ball uncertainty weights used for the H-∞ designs. The application of μ-synthesis also requires the selection of so-called D-scales. The order of rational polynomial approximations to the D-scales adds to the order of the resulting control laws. Therefore, the μ-synthesis controllers generally have higher dynamic order than the H-∞ designs.

The solution of the μ-synthesis problem involves an iterative process, D-K iteration.[9] This iterative process does not, however, converge to a unique controller. The designer must decide how many iterations are needed, whether or not the desired level of robustness (i.e., $\mu \leq 1$) can be achieved, and if the robustness of the current iterate is acceptable. Sensitivity of the D-K iteration procedure to initial conditions and parameter selections (e.g., γ and D-scale approximations) resulted in difficulty arriving at acceptable μ-synthesis controllers, but the final full-order μ-synthesis control laws did have structured singular values that were all near unity.

Control laws μ #1 and μ #2, based on the simple weights, were 31st and 29th order, respectively. These designs differ because of the choices for γ and D-scale approximations. Control law μ #3, based on the complex weights, was 35th order. Once the control laws were obtained washout filters (identical to that used for the H-∞ control laws) were again added to reject biases and low frequency disturbances. The addition of the first order washout filters further increased the controller order by two. These control laws were also too large to fit within the digital controller.

As a result, internally balanced controller order reduction[12] was once again employed to reduce the order. The final order for control laws μ #1, μ #2, and μ #3 were 22, 26, and 24, respectively. Figures 9, 10, and 11 present the frequency responses of the three reduced order μ-synthesis control laws that were tested in the wind-tunnel.

Analysis and Experimental Results

Analysis

Each of the control designs presented above were able to achieve the design objectives to various degrees. In this section, the degree to which each of the control law designs accomplished the design objectives will be discussed. All the analysis presented here was obtained using the P-Δ model in Figure 5 and the mathematical model of the BACT system presented in reference 8.

The SISO control law designs were predicted to have excellent analytical stability margins over the entire range of operating conditions, but the margins for the trailing edge flap control law were generally better than for the upper spoiler control law. Similarly, the MIMO control laws had

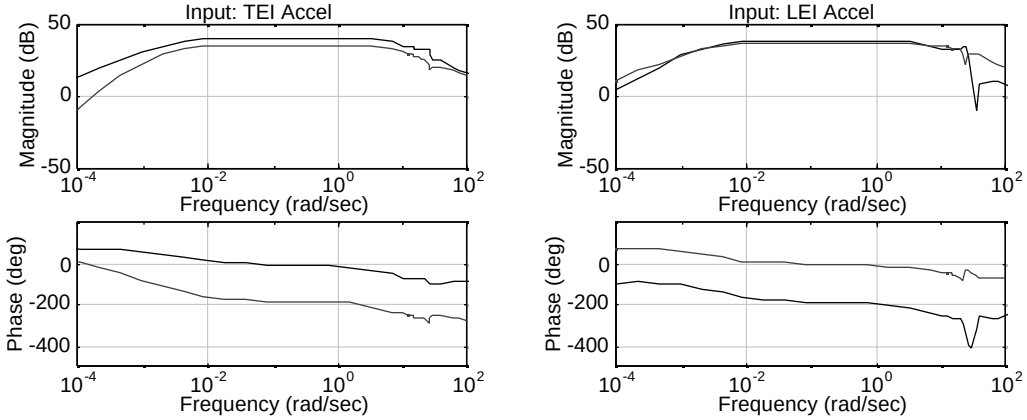

Figure 9 - μ #1 frequency response (solid - TE control, dash - LE control).

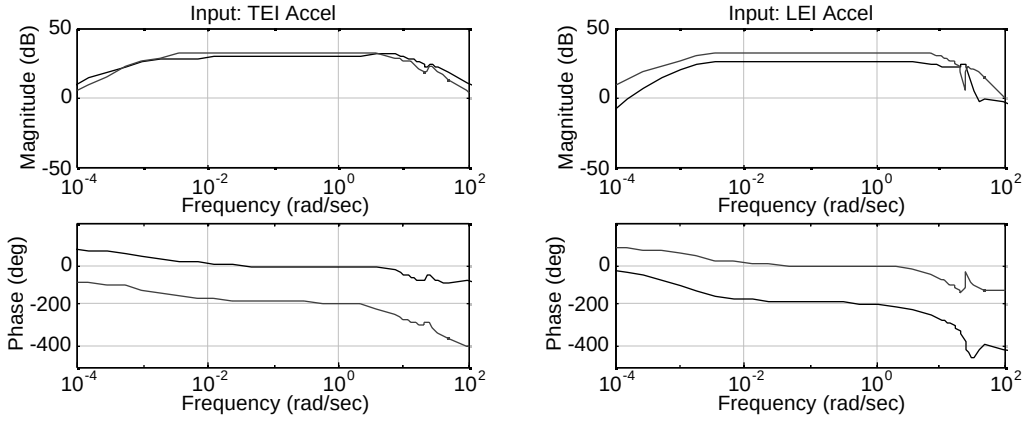

Figure 10 - μ #2 frequency response (solid - TE control, dash - LE control).

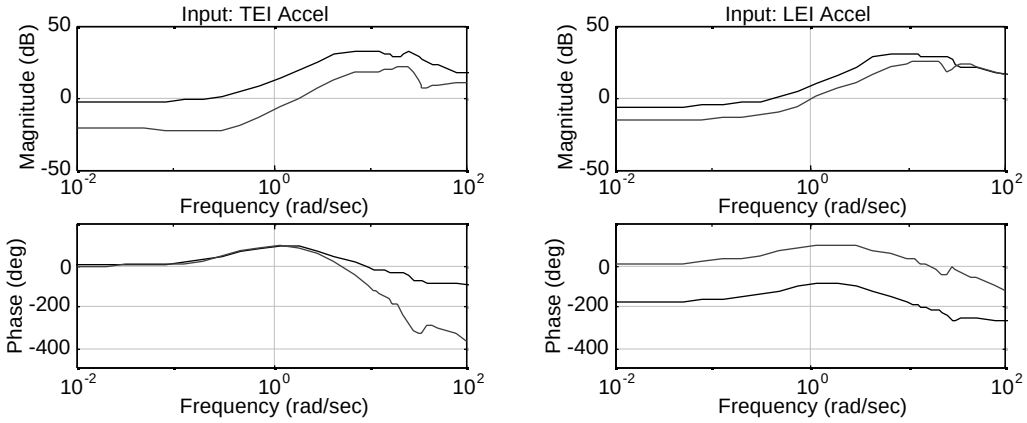

Figure 11 - μ #3 frequency response (solid - TE control, dash - LE control).

excellent predicted stability margins (as indicated by the fact that each design had structured singular values near unity). However, the process of adding washout filters and reducing the controller order affected the robustness of the MIMO control laws by reducing the stability margins relative to the full order designs.

Structured singular values, based on the simple performance and control weights, are used as a basis for stability robustness comparisons among the various controllers. Two uncertainty models were used, the one based on the averaged design model (see Figure 5) and the constant unit-ball uncertainty used to perform the H-∞ and μ-synthesis designs. Table 1 summarizes the structured singular values for the various SISO and MIMO control laws.

Notice that none of the control laws had structured singular values (SSV's) below one, which would guarantee stability subject to arbitrary uncertainties bounded in magnitude by the associated uncertainty weight. In fact, while the μ-synthesis controllers were initially designed to have SSV's of approximately one for unit uncertainty, the process of adding washout filters and reducing the controller order increased the SSV's to values above those for the H-∞ designs. However, the robustness was better than that achieved by the trailing edge, TE, and upper spoiler, US, designs or their combination, TE+US. It is also interesting to note that the μ-synthesis control law based on the more complex performance and control weights (i.e., μ #3) demonstrated the worst robustness of the MIMO designs.

Structured singular values can also provide a measure of performance robustness. Using the same weights and uncertainty models, the MIMO control laws were assessed for their ability to keep peak acceleration levels below 0.1g and peak control deflections below 1.0 degree. An SSV of unity indicates that the performance objective is met by all systems bounded by the associated uncertainty model. Table 1 summarizes the SSV's associated with performance robustness. Since the performance measure is very closely related to the stability measure the performance results parallel the stability results. The SSV's indicate that, though the specific performance objective was not met, the MIMO designs were clearly superior to the SISO designs and successfully reduced acceleration levels with acceptable control activity. Some additional real-μ analysis was performed (not shown here) that indicated the complex uncertainty was only slightly more conservative in assessing robust stability and slightily more conservative in assessing robust performance.

Simulation studies of both the SISO and MIMO control laws were also conducted. Each of the control laws maintained stability over the entire range of simulated wind-tunnel operating conditions -- $M = 0.77$, $0 < q < 225$ psf. The performance levels of all the control laws were very similar with rms accelerations on the order of 0.03 g's. In addition, the MIMO designs were

Table 1 - Predicted Robustness Properties of MIMO Controllers (M=0.77, q=175 psf)

Control Laws	Controller Order	Structured Singular Values (Stability Robustness)		Structured Singular Values (Performance Robustness)	
		Averaged Uncertainty	Unit Uncertainty	Averaged Uncertainty	Unit Uncertainty
TE	3	41	4.3	42	6.5
US	3	28	4.2	29	4.6
TE+US	6	57	5.8	57	6.2
H-∞ #1	7	11.2	1.4	11.5	1.5
H-∞ #2	12	10.8	1.3	10.9	1.4
μ #1	22	13.9	2.4	14.0	4.2
μ #2	26	10.6	1.6	10.8	2.0
μ #3	24	36	4.6	37	5.3

generally able to suppress large initial condition perturbations more effectively (i.e., shorter settling times).

One other design objective was to keep the controller order as small as possible in order to simplify the implementation and assure that the limits of the digital controller were not exceeded. This proved to be a difficult task for the MIMO designs. Order reduction was required for these controllers to fit in the digital controller (see Table 1). As a result, some of the robustness benefits of the μ-synthesis approach have been lost as is evident by the larger that unity SSV's for the reduced order controls laws evaluated with the unit-ball uncertainty.

Experimental Results

The various control laws were implemented in the BACT's digital control computer and used to control the BACT system over the entire range of wind-tunnel conditions - $0.5<M<0.95$ and $100<q<200$ psf. These conditions represent both open-loop stable and open-loop unstable conditions. All the control laws were successful in suppressing flutter and maintaining closed-loop stability when the system was open-loop stable. In addition, the acceleration levels associated with the various controllers were quite acceptable with the MIMO designs somewhat better than the SISO designs. Table 2 summarizes the performance of the various control laws in terms of rms accelerations and control surface commands for an open-loop unstable condition.

The basic difference between the various controllers was the control activity required. This was not particularly evident during normal operations since all the controllers required much less than 1.0 degree rms control inputs. However, when large oscillations were allowed to develop by disengaging the controller at an open-loop unstable condition, the control activity and system response that resulted when re-engaging the controller was significantly better for the MIMO designs. This can attributed to both the added control power associated with multiple control surfaces and the fully-coupled nature of the MIMO control laws since the MIMO control laws were superior to the combination of the two SISO control laws.

Robustness was assessed experimentally using the controller performance evaluation (CPE) tool[3] to compute generalized robustness measures from response data. Table 3 summarizes the robustness of the various control laws obtained from the CPE results in terms of the minimum singular values of the return difference matrix at the plant input and output. Note that the μ-synthesis control laws have generally better robustness than the others.

Table 2 - Experimental RMS Performance Data for the BACT Control Laws (M=0.77, q = 175 psf)

Control Law	TEI Accel. (g's)	LEI Accel. (g's)	TE Command (deg)	US Command (deg)
TE	0.033	0.042	0.35	-
US	0.038	0.045	-	0.55
TE+US	0.029	0.038	0.22	0.44
H-∞ #1	0.03	0.03	0.31	0.34
H-∞ #2	0.03	0.03	0.32	0.29
μ #1	0.03	0.03	0.20	0.28
μ #2	0.03	0.03	0.25	0.17
μ #3	0.04	0.04	0.25	0.23

Table 3 - Experimental Robustness Data for the BACT Control Laws (M=0.76-0.79, q = 174-180 psf)

Control Law	min SV @ Input	min SV @ Output
TE	0.84	0.45
US	0.36	0.08
TE+US	0.42	0.24
H-∞ #1	0.34	0.32
H-∞ #2	0.43	0.24
μ #1	0.60	0.67
μ #2	0.55	0.68
μ #3	0.40	0.29

Concluding Remarks

The H-∞ and μ-synthesis robust multivariable control design methods have been successfully applied to the problem of wing flutter suppression for a simple wind-tunnel model. These methods have been shown to result in control laws which have similar nominal performance and better stability and performance robustness than more traditional single-input/single-output designs. In addition, a constant control law was able to maintain closed-loop stability over a very wide range of (open-loop stable and unstable) wind-tunnel operating conditons.

However, some of the benefits associated with robust multivariable control design were not fully realized. Controller reduction was required to fit the control laws into the control computer and washout filters had to be added a posteriori to reject sensor biases. In addition, attempts to use uncertainty representations based on actual plant differences due to dynamic pressure variations were unsuccessful for both the H-∞ and μ-synthesis designs. Each of these post design modications reduced the performance and robustness of the multivariable control law design. Additional research is required to overcome these limitations.

Beside the demonstration of robust multivariable control for flutter suppression the BACT project has had several other valuable outcomes. Spoilers have been demonstrated to be an excellent option for applications to active flutter suppression. The BACT wind-tunnel model system has proven to be a very reliable active control testbed and offers excellent opportunities for future research. The mathematical model of the BACT system used for control system design has been extensively documented and is available for educational and research applications. And the extensive database that has been collected is available to further develop aeroelastic modeling methods and control system design methods.

Acknowledgment

The author wishes to acknowledge Vivek Mukhopadhyay, Rob Scott, Sheri Hoadley, Carol Wieseman, Robert Bennett, Robert Sleeper, and the entire BACT team without whose help this work could not have been accomplished.

References

[1] Durham, M.H.; Keller, D.F.; Bennett, R.M.; and Wieseman, C.D.: A Status Report on a Model for Benchmark Active Controls Testing. AIAA Paper No. 91-1011.

[2] Bennett. R.M.; Eckstrom, C.V.; et al..: The Benchmark Aeroelastic Models Program - Description and Highlights of Initial Results. NASA TM-104180, Dec. 1991.

[3] Wieseman, C.D.; Hoadley, S.T.; and McGraw, S.M.: On-Line Analysis Capabilities Developed to Support Active Flexible Wing Wind-Tunnel Model. Journal of Aircraft. Vol. 23, No. 1. pp. 39-44. Jan.-Feb. 1995.

[4] Waszak, Martin R.; and Srinathkumar, S.: Flutter Suppression for the Active Flexible Wing: A Classical Design. Journal of Aircraft. Vol. 32, No. 1, pp. 61-67. January-February, 1995.

[5] Rivera, Jr., J.A.; Dansberry, B.E.; Durham, M.H.; Bennett, R.M.; and Silva, W.A.: Pressure Measurements on a Rectangular Wing with a NACA 0012 Airfoil During Conventional Flutter. NASA TM-104211, July 1992.

[6] Staff of the Aeroelasticity Branch: The Langley Transonic Dynamics Tunnel. Langley Working Paper, LWP-799, September 23, 1969.

[7] Scott, R.C.; Hoadley, S.T.; Wieseman, C.D.; and Durham, M.H.: The Benchmark Active Controls Technology Model Aerodynamic Data. AIAA Paper No. 97-0829. 35Th Aerospace Sciences Meeting and Exhibit. Reno, NV. January 6-10, 1997.

[8] Waszak, M.R.: Modeling the Benchmark Active Control Technology Wind-Tunnel Model for Application to Flutter Suppression. AIAA Paper No. 96-3437. AIAA Atmospheric Flight Mechanics Conference. San Diego, CA. July 29-31, 1996.

[9] Balas, GJ.; Doyle, J.C.; Glover, K.; Packard, A.; and Smith, R.: μ-Analysis and Synthesis Toolbox (for Use with MATLAB) - User's Guide. The MathWorks, Inc. and MUSYN, Inc. July 1993.

[10] Doyle, J.C. and Stein, G.: Multivariable Feedback Design: Concepts for a Classical / Modern Synthesis. IEEE Trans. On Auto. Control, Vol. AC-26, No. 1, February 1981.

[11] Anderson, M.R.: Linear Design Models for Robust Control Synthesis. AIAA Paper No. 89-3454. AIAA Guidance, Navigation, and Controls Conference. Boston, MA. August 1989. Pp. 263-270.

[12] Bacon, B.J.; and Schmidt, D.K.: Multivariable Frequency-Weighted Order Reduction. Journal of Guidance, Control, and Dynamics, Volume 12, No. 1, January-February 1989.